Quantum Telecommunication Based on Atomic Cascade Transitions

T. Chanelière, D. N. Matsukevich, S. D. Jenkins, T. A. B. Kennedy, M. S. Chapman, and A. Kuzmich
School of Physics, Georgia Institute of Technology, Atlanta, Georgia 30332-0430, USA
(Received 9 January 2006; published 10 March 2006)

A quantum repeater at telecommunications wavelengths with long-lived atomic memory is proposed, and its critical elements are experimentally demonstrated using a cold atomic ensemble. Via atomic cascade emission, an entangled pair of 1.53 μm and 780 nm photons is generated. The former is ideal for long-distance quantum communication, and the latter is naturally suited for mapping to a long-lived atomic memory. Together with our previous demonstration of photonic-to-atomic qubit conversion, both of the essential elements for the proposed telecommunications quantum repeater have now been realized.

DOI: 10.1103/PhysRevLett.96.093604 PACS numbers: 42.50.Dv, 03.65.Ud, 03.67.Hk

A quantum network would use the resources of distributed quantum-mechanical entanglement, thus far largely untapped, for the communication and processing of information via qubits [1,2]. Significant advances in the generation, distribution, and storage of qubit entanglement have been made using laser manipulation of atomic ensembles, including atom-photon entanglement and matter-light qubit conversion [3], Bell inequality violation between a collective atomic qubit and a photon [4], and light-matter qubit conversion and entanglement of remote atomic qubits [5]. In each of these works, photonic qubits were generated in the near-infrared spectral region. In related developments, entanglement of an ultraviolet photon with a trapped ion [6] and of a near-infrared photon with a single trapped atom [7] have been demonstrated. Heterogeneous quantum network schemes that combine single-atom and collective atomic qubits are being actively pursued [8]. However, photons in the ultraviolet to the near-infrared range are not suited for long-distance transmission over optical fibers due to high losses.

In this Letter, we propose a telecommunications wavelength quantum repeater based on cascade atomic transitions in either (1) a single atom or (2) an atomic ensemble. We will first discuss the latter case, with particular reference to alkali metals. Such ensembles, with long-lived ground level coherences can be prepared in either the solid [9] or gas [4] phase. For concreteness, we consider a cold atomic vapor confined in high vacuum. The cascade transitions may be chosen so that the photon (signal) emitted on the upper arm has telecommunication range wavelength, while the second photon (idler), emitted to the atomic ground state, is naturally suited for mapping into atomic memory. Experimentally, we demonstrate phase-matched cascade emission in an ensemble of cold rubidium atoms using two different cascades: (a) at the signal wavelength $\lambda_s = 776$ nm, via the $5s_{1/2} \rightarrow 5d_{5/2}$ two-photon excitation; (b) at $\lambda_s = 1.53$ μm, via the $5s_{1/2} \rightarrow 4d_{5/2}$ two-photon excitation. We observe polarization entanglement of the emitted photon pairs and superradiant temporal profiles of the idler field in both cases.

We now describe our approach in detail and at the end we will summarize an alternative protocol for single atoms.

Step (A).—As illustrated in Fig. 1(a), the atomic sample is prepared in level $|a\rangle$, e.g., by means of optical pumping. For an atomic ensemble qubit, an incoherent mixture of Zeeman states can be sufficient [4]. The upper level $|d\rangle$, which may be of either s or d type, can be excited either by one- or two-photon transitions, the latter through an intermediate level $|c\rangle$. The advantage of two-photon excitation is that it allows for noncollinear phase matching of signal and idler photons; single-photon excitation is forbidden in electric dipole approximation and phase-matched emission is restricted to a collinear geometry (this argument implicitly assumes that the refractive index of the vapor is approximately unity). Ideally the excitation is two-photon detuned from the upper level $|d\rangle$, creating a virtual excitation.

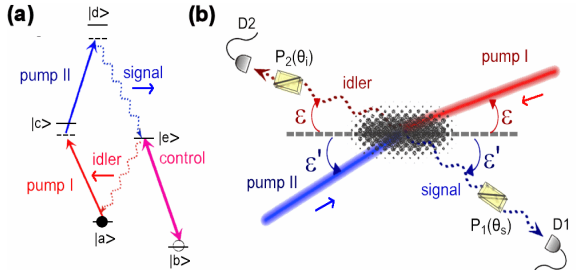

FIG. 1 (color online). (a) The atomic structure for the proposed cascade emission scheme involving excitation by pumps I and II. Pump II and the signal photons lie in the telecommunication wavelength range when a suitable level of orbital angular momentum $L = 0$ or $L = 2$ is used as level $|d\rangle$. For atomic rubidium, the signal wavelength is 1.32 μm ($6s_{1/2} \rightarrow 5p_{1/2}$ transition), 1.37 μm ($6s_{1/2} \rightarrow 5p_{3/2}$ transition), 1.48 μm ($4d_{3/2(5/2)} \rightarrow 5p_{1/2}$ transition), 1.53 μm ($4d_{3/2(5/2)} \rightarrow 5p_{3/2}$ transition). For atomic cesium, the signal wavelength is 1.36 μm ($7s_{1/2} \rightarrow 6p_{1/2}$ transition), 1.47 μm ($7s_{1/2} \rightarrow 6p_{3/2}$ transition). For Na and K the corresponding wavelengths are in the 1.1–1.4 μm range. (b) Schematic of experimental setup based on ultracold ^{85}Rb atomic gas. For $\lambda_s = 776$ nm, phase matching results in the angles $\varepsilon' \approx \varepsilon \approx 1°$, while for $\lambda_s = 1.53$ μm, $\varepsilon' \approx 2\varepsilon \approx 2°$. P_1 and P_2 are polarizers; $D1$ and $D2$ are detectors.

Step (B).—Scattering via the upper level $|d\rangle$ to ground level $|a\rangle$ through the intermediate level $|e\rangle$ (where $|e\rangle$ may coincide with $|c\rangle$) results in the cascaded emission of signal and idler fields. The signal field, which is emitted on the upper arm, has a temporal profile identical to that of the laser excitation as a consequence of the large two-photon detuning. As noted earlier, the wavelength of this field lies in the 1.1–1.6 μm range, depending on the alkali-metal transition used. The signal field can be coupled to an optical fiber (which may have losses as low as 0.2 dB/km) and transmitted to a remote location.

The temporal profile of the idler field can be much shorter than the single-atom spontaneous decay time t_s of the intermediate level. Under the conditions of a large Fresnel number of the exciting laser fields, the decay time is of order $t_s/d_{\rm th}$, characteristic of superradiance [10,11]. Here $d_{\rm th} \approx 3n\lambda^2 l/(8\pi)$ is the optical thickness, where λ is the wavelength, n is the number density, and l is the length of the sample.

The direction of the idler field is determined by the phase matching condition $\vec{k}_1 + \vec{k}_2 = \vec{k}_s + \vec{k}_i$, where $\vec{k}_1$ and $\vec{k}_2$ are the wave vectors of the laser fields I and II, respectively. Under conditions of phase matching, collective enhancement causes emission of the idler photon correlated with a return of the atom into the Zeeman state from which it originated [4]. The fact that the atom begins and ends the absorption-emission cycle in the same state is essential for strong signal-idler polarization correlations. The reduced density operator for the field, taking into account collective enhancement, was derived in Ref. [12]:

$$\hat{\rho}(t) \approx [1 + \sqrt{\epsilon}\hat{A}_2^\dagger(t)]\hat{\rho}_{\rm vac}[1 + \sqrt{\epsilon}\hat{A}_2(t)], \qquad (1)$$

where $\hat{\rho}_{\rm vac}$ is the vacuum state of the field, $\hat{A}_2^\dagger(t)$ is a time-dependent two-photon creation operator for the signal and idler fields, and $\epsilon \ll 1$. For linearly polarized pumps with parallel (vertical) polarizations, we find in the long-time limit

$$\hat{A}_2^\dagger(t) = (\cos\chi)\hat{a}_H^\dagger\hat{b}_H^\dagger + (\sin\chi)\hat{a}_V^\dagger\hat{b}_V^\dagger, \qquad (2)$$

where χ is determined by Clebsch-Gordan coupling coefficients [12], $\hat{a}_{H(V)}^\dagger$ and $\hat{b}_{H(V)}^\dagger$ are creation operators for a horizontally (vertically) polarized signal and idler photon, respectively. For the hyperfine level configuration $F_a = 3 \rightarrow F_c = 4 = F_e \rightarrow F_d = 5$, and for an unpolarized atomic sample, we find $\sin\chi = 2\cos\chi = 2/\sqrt{5}$.

Step (C).—The photonic qubit is encoded in the idler field polarization. Photonic-to-atomic qubit conversion was achieved in Ref. [5]. Such conversion can be performed either within the same ensemble or in a suitably prepared adjacent ensemble or pair of ensembles. In either case, a strong laser control beam is required to couple the other ground hyperfine level $|b\rangle$ to the intermediate level $|e\rangle$. Collective excitations involving two orthogonal hyperfine coherences serve as the logical states of the atomic qubit [3–5].

Experiment.—We observe phase-matched cascade emission of entangled photon pairs, using samples of cold ^{85}Rb atoms, for two different atomic cascades: (a) at $\lambda_s =$ 776 nm, via the $5s_{1/2} \rightarrow 5d_{5/2}$ two-photon excitation; (b) at $\lambda_s = 1.53$ μm, via the $5s_{1/2} \rightarrow 4d_{5/2}$ two-photon excitation. The investigations are carried out in two different laboratories using similar setups, Fig. 1(b). A magneto-optical trap (MOT) of ^{85}Rb provides an optically thick cold atomic cloud. The atoms are prepared in an incoherent mixture of the level $|a\rangle$, which corresponds to the $5s_{1/2}$, $F_a = 3$ ground level, by means of optical pumping. The intermediate level $|c\rangle = |e\rangle$ corresponds to the $5p_{3/2}$, $F_c = 4$ level of the D_2 line at 780 nm, and the excited level $|d\rangle$ represents (a) the $5d_{5/2}$ level with $\lambda_s =$ 776 nm, or (b) the $4d_{5/2}$ level with $\lambda_s = 1.53$ μm. Atomic level $|b\rangle$ corresponds to $5s_{1/2}$, $F_b = 2$, and could be used to implement the light-to-matter qubit conversion [5].

The trapping and cooling light as well as the quadrupole magnetic field of the MOT are switched off for the 2 ms duration of the measurement. The ambient magnetic field is compensated by three pairs of Helmholtz coils. Counter-propagating pumps I (at 780 nm) and II (at 776 nm or 1.53 μm), tuned to two-photon resonance for the $|a\rangle \rightarrow |d\rangle$ transition are focused into the MOT using the off-axis, counterpropagating geometry of Harris and co-workers [13]. This two-photon excitation induces phase-matched signal and idler emission.

With quasi-cw pump fields, we perform photoelectric coincidence detection of the signal and idler fields. The latter are directed onto single-photon detectors $D1$ and $D2$. For $\lambda_s = 1.53$ μm, the signal field is coupled into 100 m of single-mode fiber, and detector $D1$ [cooled (In,Ga)As photon counting module] is gated using the output pulse of silicon detector $D2$. The delay between the electronic pulses from $D1$ and $D2$ is determined with 1 ns time resolution.

We measure the stationary signal-idler intensity correlation function $G_{\rm si}(\tau) = \langle \mathcal{T} : \hat{I}_s(t)\hat{I}_i(t+\tau) : \rangle$, where the notation $\mathcal{T}$: denotes time and normal ordering of operators, and $\hat{I}_s$ and $\hat{I}_i$ are the signal and idler intensity operators, respectively [11]. Results for (a) $\lambda_s = 776$ nm and (b) $\lambda_s =$ 1.53 μm are presented in Figs. 2 and 3, respectively. In particular, the measured correlation functions are shown in Figs. 2(a), 2(b), and 3(a). The correlation function shown in Fig. 2(a) exhibits quantum beats due to the two different hyperfine components of the $5p_{3/2}$ level [14]. The correlation times are consistent with superradiant scaling $\sim t_s/d_{\rm th}$, Fig. 2(c), where $t_s \approx 27$ ns for the $5p_{3/2}$ level [10].

In order to investigate polarization correlations of the signal and idler fields, they are passed through polarizers P_1 (set at angle θ_s) and P_2 (set at angle θ_i), respectively, as shown in Fig. 1(b). We integrate the time-resolved counting rate over a window ΔT centered at the maximum of the signal-idler intensity correlation function $G_{\rm si}(\tau)$, with (a) $\Delta T = 6$ ns for $\lambda_s = 776$ nm, and (b) $\Delta T = 1$ ns for $\lambda_s =$ 1.53 μm. The resulting signal-idler coincidence rate

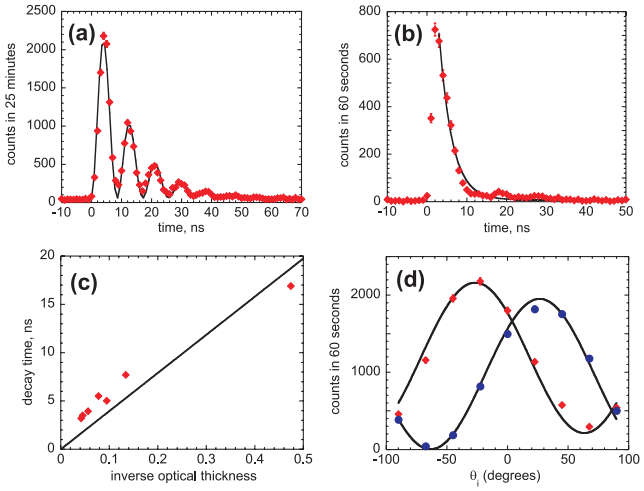

FIG. 2 (color online). (a) Count rate proportional to the signal-idler intensity correlation function G_{si} as a function of signal-idler delay τ, $|d\rangle = |5d_{5/2}, F = 4\rangle$. The quantum beats are associated with 120 MHz hyperfine splitting, $F = 3$ and 4, of the $5p_{3/2}$ level [14]. The solid curve is a fit of the form $\beta + A \times \exp(-t/\alpha)\sin^2(\pi\Omega t)$, where $\beta = 63$, $A = 2972$, $\alpha = 11$ ns, and $\Omega = 117$ MHz are adjustable parameters. (b) Same as (a), but for $|d\rangle = |5d_{5/2}, F = 5\rangle$. Since this state can only decay though the $F = 4$ component of the $5p_{3/2}$ level, there are no quantum beats. The solid curve is an exponential fit with decay time of 3.2 ns. (c) The measured decay time vs the inverse measured optical thickness. (d) Measured coincidence fringes for $\theta_s = 45°$ (red diamonds) and $\theta_s = 135°$ (blue circles). The solid curves are fits based on Eqs. (1) and (2), with $\cos\chi = 1/\sqrt{5}$.

$C(\theta_s, \theta_i)$ exhibits sinusoidal variation as a function of the polarizers' orientations, as shown in Figs. 2(d) and 3(b). In order to verify the predicted polarization entanglement, we check for violation of Bell's inequality $S \leq 2$ [11,15,16]. We first calculate the correlation function $E(\theta_s, \theta_i)$, given by

$$\frac{C(\theta_s, \theta_i) + C(\theta_s^\perp, \theta_i^\perp) - C(\theta_s^\perp, \theta_i) - C(\theta_s, \theta_i^\perp)}{C(\theta_s, \theta_i) + C(\theta_s^\perp, \theta_i^\perp) + C(\theta_s^\perp, \theta_i) + C(\theta_s, \theta_i^\perp)},$$

where $\theta^\perp = \theta + \pi/2$, and $S = |E(\theta_s, \theta_i) + E(\theta_s', \theta_i)| + |E(\theta_s, \theta_i') - E(\theta_s', \theta_i')|$.

Measured values of $E(\theta_s, \theta_i)$, using the set of angles θ_s, θ_i, chosen to maximize the violation of Bell's inequality, are presented in Table I. We find (a) $S = 2.185 \pm 0.025$ for $\lambda_s = 776$ nm, and (b) $S = 2.132 \pm 0.036$ for $\lambda_s = 1.53$ μm, consistent with polarization entanglement of signal and idler fields in both cases. The entangled two-photon state of Eqs. (1) and (2), for $\sin\chi = 2/\sqrt{5}$, has a substantial degree of asymmetry. If oppositely, circularly, polarized pumps I and II were used, the corresponding two-photon state would be symmetric with $\sin\chi = \cos\chi = 1/\sqrt{2}$ [12].

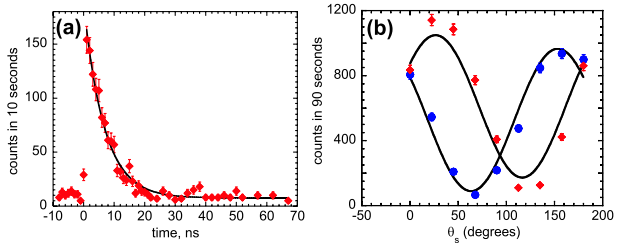

FIG. 3 (color online). (a) Same as Figs. 2(a) and 2(b), but for $|d\rangle = |4d_{5/2}, F = 5\rangle$. The solid curve is an exponential fit with decay time of 6.7 ns. (b) Measured coincidence fringes for $\theta_i = 45°$ (red diamonds) and $\theta_i = 135°$ (blue circles). The solid curves are fits based on Eqs. (1) and (2), with $\cos\chi = 1/\sqrt{5}$.

The quantum repeater protocol involves sequential entanglement swapping via Hong-Ou-Mandel (HOM) interference followed by coincidence detection [2,11]. High-visibility HOM interference requires that the signal and idler photon wave packets have no entanglement in the time or frequency domains [17]. This may be achieved with excitation pulses that are far detuned from two-photon resonance and with pulse lengths much shorter than the superradiant emission time t_s/d_{th} of level $|e\rangle$.

The idler field qubit is naturally suited for conversion into an atomic qubit encoded into the collective hyperfine coherence of levels $|a\rangle = |5s_{1/2}, F = 3\rangle$ and $|b\rangle = |5s_{1/2}, F = 2\rangle$. To perform such conversion, either the same or another similar ensemble or pair of ensembles could be employed [5]. A time-dependent control laser field resonant on the $|b\rangle = |5s_{1/2}, F = 2\rangle \leftrightarrow |e\rangle = |5p_{3/2}, F = 3\rangle$ transition could selectively convert one of the two frequency components of the idler field, shown in Fig. 2(a), into a collective atomic qubit. Pulsed excitation should be used in order to enable the synchronization of the idler qubit and the control laser. Numerical simulations show that light conversion and subsequent retrieval can be done with good efficiency for moderate optical thicknesses (Fig. 4), even though the idler field temporal profile is shorter than those employed in Ref. [5] (compare with Fig. 3 in Ref. [18]). In order to convert a qubit, one could either optically pump the atoms into an $m = 0$ Zeeman state [5], or employ a distinct ensemble for each of the polarization components of the idler field [3].

The basic protocols we have outlined can also be applied to single alkali atom emitters. Similar cascade decays in single atoms were used in early experiments demonstrating

TABLE I. Measured correlation function $E(\theta_s, \theta_i)$ and S for $\lambda_s = 776$ nm and $\lambda_s = 1.53$ μm.

λ_s	θ_s	θ_i	$E(\theta_s, \theta_i)$
776 nm	0°	−67.5°	-0.670 ± 0.011
	45°	−22.5°	-0.503 ± 0.013
	0°	−22.5°	0.577 ± 0.012
	45°	−67.5°	-0.434 ± 0.014
			$S = 2.185 \pm 0.025$
1.53 μm	22.5°	45°	-0.554 ± 0.027
	67.5°	0°	-0.682 ± 0.027
	22.5°	0°	0.473 ± 0.024
	67.5°	45°	-0.423 ± 0.029
			$S = 2.132 \pm 0.036$

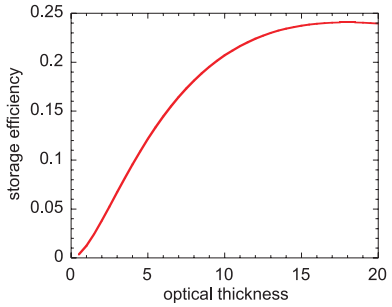

FIG. 4 (color online). Efficiency of storage and subsequent retrieval of a coherent idler field with decay time of 6 ns in an auxiliary atomic ensemble, obtained by numerical integration of the Maxwell-Bloch equations [12,18,23]. This efficiency is independent of the storage time as long as the latter is much shorter than the atomic memory time. The control field Rabi frequency is chosen to be $3/t_s$, and is turned off smoothly between 10 and 30 ns after the idler enters the auxiliary ensemble. For these parameters the maximum efficiency is limited since the spectral width of the idler pulse is much wider than the transparency window. However, increased storage efficiency is found using larger control field intensities [12].

violation of local realism [19] and single-photon generation [20]. For alkali-metal atoms, it is necessary to optically pump the atom into a single Zeeman state, e.g., $m = 0$, of level $|a\rangle$. A virtual excitation of a single Zeeman state of level $|d\rangle$ is created with short laser pulses. Coherent Raman scattering to level $|e\rangle$ results in atom-photon polarization entanglement. In order to prevent spontaneous decay of the level $|e\rangle$, a control field π pulse is applied immediately after the application of the two-photon excitation, transferring the atomic qubit into the ground state where it could live for a long time. It is important that the π-pulse duration is shorter than the spontaneous lifetime of level $|e\rangle$. Two-photon interference and photoelectric detection of signal photons produced by two remote single-atom nodes would result in entanglement of these remote atomic qubits [21]. Qubit detection for single atoms can be achieved with nearly unit efficiency and in a time as short as 50 μs [6]. Such high efficiency and speed lead to the possibility of a loophole-free test of Bell's inequality, for atoms separated by about 30 kilometers. Cascaded entanglement swapping between successive pairs of remote entangled atomic qubits may be achieved via local coupling of one of the atoms from the first pair and its neighboring partner from the following pair [22].

We also point out that the cascade level scheme employed here can be used to convert a telecommunications photon into a near-infrared photon using four-wave mixing. This could potentially be useful because single-photon detectors for the visible and near-infrared currently have much higher quantum efficiency, and much lower dark count probability than practically viable [e.g., (In,Ga)As] detectors used at telecommunication wavelengths.

In summary, we have proposed a practical telecommunication quantum repeater scheme based on cascade transitions in alkali-metal atoms. We have generated entanglement of a pair of 1.53 μm and 780 nm photons using an ensemble of ultracold rubidium atoms. Combined with our recent demonstration of light-to-matter qubit conversion [5], key steps of our proposal have been taken. It is now necessary to focus on increased atomic memory lifetimes as these represent a limiting factor in long-distance quantum communication.

We thank Luis Orozco for fruitful discussions, particularly for pointing out the telecommunications transitions in rubidium [24]. We also thank Prem Kumar for helpful interactions, and Shau-Yu Lan for experimental assistance. We gratefully acknowledge the generous loan of a (In,Ga)As single-photon detector by Henry Yeh and BBN Technologies. This work was supported by the Office of Naval Research, National Science Foundation, NASA, Alfred P. Sloan Foundation, and Cullen-Peck Foundation.

[1] H.-J. Briegel *et al.*, Phys. Rev. Lett. **81**, 5932 (1998); W. Duer *et al.*, Phys. Rev. A **59**, 169 (1999).
[2] L.-M. Duan *et al.*, Nature (London) **414**, 413 (2001).
[3] D. N. Matsukevich and A. Kuzmich, Science **306**, 663 (2004); similar results were reported a year later in C. W. Chou *et al.*, Nature (London) **438**, 828 (2005).
[4] D. N. Matsukevich *et al.*, Phys. Rev. Lett. **95**, 040405 (2005).
[5] D. N. Matsukevich *et al.*, Phys. Rev. Lett. **96**, 030405 (2006).
[6] B. B. Blinov *et al.*, Nature (London) **428**, 153 (2004); D. L. Moehring *et al.*, Phys. Rev. Lett. **93**, 090410 (2004).
[7] J. Volz *et al.*, Phys. Rev. Lett. **96**, 030404 (2006).
[8] M. Saffman and T. G. Walker, Phys. Rev. A **72**, 042302 (2005); D. D. Yavuz *et al.*, quant-ph/0509176.
[9] M. Arndt *et al.*, Phys. Rev. Lett. **74**, 1359 (1995).
[10] N. E. Rehler and J. H. Eberly, Phys. Rev. A **3**, 1735 (1971); R. Friedberg and S. R. Hartmann, *ibid.* **13**, 495 (1976).
[11] L. Mandel and E. Wolf, *Optical Coherence and Quantum Optics* (Cambridge University Press, Cambridge, England, 1995).
[12] S. D. Jenkins *et al.* (to be published).
[13] V. Balic *et al.*, Phys. Rev. Lett. **94**, 183601 (2005).
[14] F. Vrehen, H. M. J. Hikspoors, and H. M. Gibbs, Phys. Rev. Lett. **38**, 764 (1977).
[15] D. F. Walls and G. J. Milburn, *Quantum Optics* (Springer-Verlag, Berlin, 1994).
[16] J. F. Clauser *et al.*, Phys. Rev. Lett. **23**, 880 (1969).
[17] J. D. Franson, Phys. Rev. Lett. **62**, 2205 (1989); D. Branning *et al.*, *ibid.* **83**, 955 (1999); C. K. Law, I. A. Walmsley, and J. H. Eberly, *ibid.* **84**, 5304 (2000).
[18] T. Chanelière *et al.*, Nature (London) **438**, 833 (2005).
[19] A. Aspect, P. Grangier, and G. Roger, Phys. Rev. Lett. **47**, 460 (1981).
[20] P. Grangier, G. Roger, and A. Aspect, Europhys. Lett. **1**, 173 (1986).
[21] C. Cabrillo *et al.*, Phys. Rev. A **59**, 1025 (1999).
[22] L.-M. Duan *et al.*, Quantum Inf. Comput. **4**, 165 (2004).
[23] S. D. Jenkins *et al.*, Phys. Rev. A **73**, 021803(R) (2006).
[24] E. Gomez *et al.*, Phys. Rev. A **72**, 012502 (2005).